Structural homology between bamboo mosaic virus and its satellite RNAs in the 5'untranslated region

Chen, S.C.; Desprez, A.; Olsthoorn, R.R.C.L.

Journal of General Virology (2010), **91**, 782–787 **DOI** 10.1099/vir.0.015941-0

Short Communication

Structural homology between bamboo mosaic virus and its satellite RNAs in the 5′untranslated region

Shih-Cheng Chen, Adeline Desprez and René C. L. Olsthoorn

Leiden Institute of Chemistry, Department of Molecular Genetics, PO Box 9502, 2300 RA Leiden, The Netherlands

Correspondence
René C. L. Olsthoorn
olsthoor@chem.leidenuniv.nl

Received 26 August 2009
Accepted 11 November 2009

A structural element was identified in the 5′-proximal sequence of the bamboo mosaic virus (BaMV) RNA. Mutational analysis of the hairpin showed that disruptions of the secondary structure or substitutions of the loop sequences resulted in reduced accumulation of BaMV genomic RNA. Phylogenetic analysis further suggested the presence of structural homologues of this hairpin in all other potexviruses. In addition, remarkable structural homology was discovered between the BaMV hairpin and a stem–loop in the 5′untranslated region of satellite RNAs responsible for attenuation of BaMV in co-infected plants. The role of this homology in the helper–satellite interaction is discussed.

Bamboo mosaic virus (BaMV) is a plant virus of the genus *Potexvirus* with a positive-sense RNA genome of 6366 nt, comprising five open reading frames (ORFs) (Lin *et al.*, 1994). Infections by BaMV are frequently associated with the presence of satellite (sat) RNAs, some of which may reduce accumulation of BaMV RNA and attenuate BaMV-induced symptoms in co-infected plants (Hsu *et al.*, 1998).

The 140 nt 3′untranslated region (UTR) of BaMV genomic RNA (gRNA) is composed of a pseudoknot structure involving the poly-A tail, a stem–loop structure harbouring a conserved hexamer motif and a cloverleaf-like structure formed by three adjacent hairpins (Cheng & Tsai, 1999; Tsai *et al.*, 1999). These structural elements have been implicated in the initiation of minus-strand synthesis by the viral RNA-dependent RNA polymerase (Huang *et al.*, 2001; Cheng *et al.*, 2002). However, structural elements in the 5′UTR of BaMV gRNA that potentially play roles in replication and/or translation have not been investigated in detail, although two stem–loop structures in the corresponding region of the negative-strand RNA have been suggested to be involved in positive-strand RNA synthesis (Lin *et al.*, 2005).

Using Mfold (Zuker, 2003), a large stem–loop structure was predicted in the 5′ 117 nt of BaMV positive-strand RNA (Fig. 1a). To verify the secondary structure of the predicted hairpin, in particular the upper part (nt 53–99), a transcript of approximately 1000 nt was synthesized by *in vitro* transcription of a DNA template obtained by PCR amplification of a full-length cDNA of BaMV-S (Lin *et al.*, 2004). Purified transcripts were probed with enzymes and chemicals, and analysed by denaturing gel-electrophoresis using an RNA sequencing ladder as reference, as described previously (Chen *et al.*, 2007b).

Fig. 1(b) shows that nt C80, C77, A71, A70, C69, A68, C52, A51, A50 and A41 are strongly reactive to dimethyl sulfate (DMS) while A42, A57, A58, C86 and A90 are weakly reactive. Interestingly, the absence of strong modification on C63, C64, C89 and A90 (Fig. 1b) could indicate that the C : C and the C : A mismatches in stem-II (Fig. 1a) potentially form non-Watson–Crick base pairs, as had been found in the turnip yellow mosaic virus (TYMV) 5′ hairpins (Hellendoorn *et al.*, 1997; Bink *et al.*, 2002). Nuclease S1 recognized nt A68–U73 in internal loop (IL)-I and U78 in the apical loop (AL). To some extent, U60 and U62 in stem-II are slightly susceptible to nuclease S1, suggesting that the region around the start codon is not strongly base paired. The only G residue that was recognized by RNase T1 was G79 in AL (Fig. 1d). Cuts by nuclease V1, which recognizes double-stranded regions, were observed near C56 and C55 (Fig. 1c). The absence of cuts in other, supposedly, double-stranded regions could be due to the fact that the nuclease V1 that was used is only active on stem regions that consist of more than 6 bp (Lowman & Draper, 1986). On the whole, the structural probing data are in good agreement with the proposed secondary structure for the top 30 nt (Fig. 1a).

To study the possible importance of the 5′ hairpin in the replication of BaMV, several mutants were constructed (Fig. 2a), and accumulation of their positive strand RNA in *Nicotiana benthamiana* plants was assayed by semiquantitative RT-PCR (Fig. 2b). The mutations were introduced into pBaMV-S (Lin *et al.*, 2004) by site-directed mutagenesis using a two-step PCR. The constructed mutants were verified by DNA sequencing and subsequently used for the synthesis of capped and poly-adenylated transcripts *in vitro*; the sequence for the poly-A tail is contained within the plasmid. After removing DNA templates, these infectious transcripts were applied to *N. benthamiana* plants as described by Hsu *et al.* (1998). Briefly, three 1-month-old *N. benthamiana* plants were used, of which two

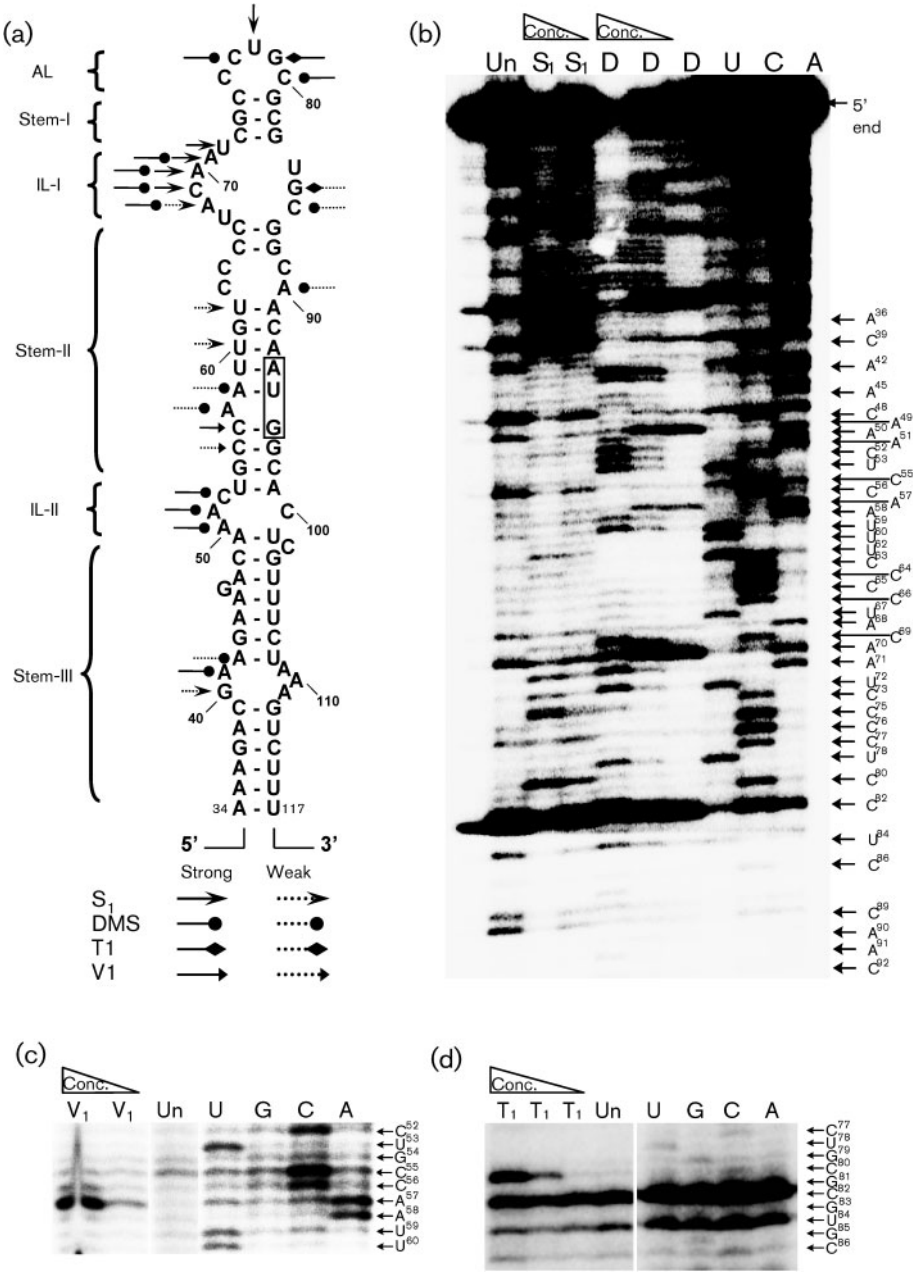

Fig. 1. Secondary structure of the BaMV 5′-proximal sequence. (a) Proposed model of the stem–loop structure around the start of ORF1 in BaMV RNA with indications of strong and weak hits by probing enzymes or chemicals. The AUG start codon of ORF1 is boxed. (b) Structure probing by DMS (lanes D) and nuclease S1 (lanes S_1) analysed by primer extension. Un, Untreated transcripts; lanes U, C and A, dideoxy sequencing using BaMV RNA. Structure probing with nuclease V_1 and RNase T_1 are shown in (c) and (d), respectively, with an additional G sequencing lane.

leaves were inoculated for each inoculation. Seven days after inoculation, infected leaves were harvested and the total RNA was isolated using RNeasy kit (Qiagen). Purified total RNA was subjected to semiquantitative RT-PCR to determine the relative amount of the viral gRNA in total RNA extracts. First strand cDNA synthesis was carried out with 0.4 μg total RNA and oligonucleotide RT-2 (5′-GGCCGCTTTAGACTCCACCCGG-3′, complementary to nt 828–807) which is specific to BaMV gRNA. Subsequently, serial dilutions of cDNA were amplified by PCR with oligonucleotide RT-3 (5′-GTACCCTCT-CGAGACTATCTACC-3′, complementary to BMV gRNA nt 468–490) as a forward primer for 24 cycles. Each amplified reaction was separated by electrophoresis for comparison of the relative accumulation of the BaMV gRNA (Fig. 2).

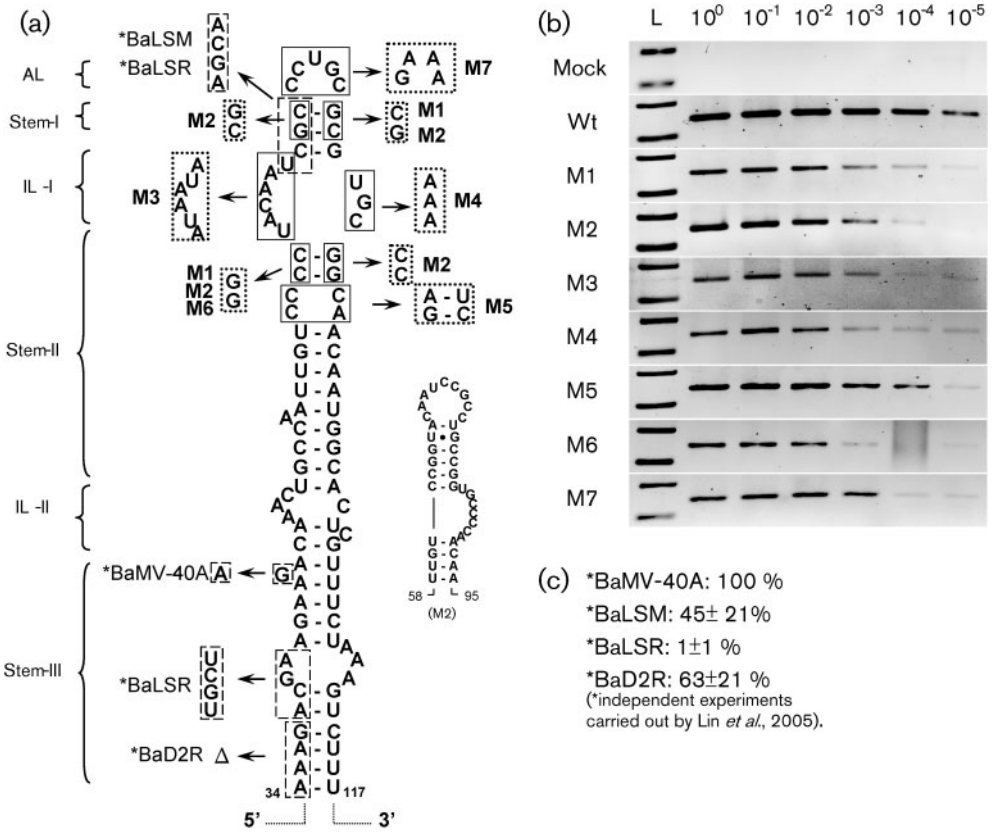

Fig. 2. Mutational analysis of the 5′ stem–loop structure of BaMV. (a) The boxed nucleotides were substituted in positive-strand BaMV gRNA with the nucleotides for each mutant indicated by dotted line boxes (this study), while mutants with sequence substitutions or deletion (Δ) in negative-strand RNA are indicated by a dashed line box (Lin *et al.*, 2005). An alternative fold for the upper part of the hairpin in mutant M2 is shown. (b) Semiquantitative PCR showing amplification of the approximately 360 bp products after sequential dilution of first strand cDNA. Mock, Control RT-PCR on mock-inoculated *N. benthamiana* plants. A DNA size ladder, 300 and 400 bp (lane L), was included in the electrophoresis. (c) The accumulation of positive-strand RNA in the mutants studied by Lin *et al.* (2005).

In mutant M1, two base pairs in stem-I and stem-II were disrupted, while in M6, only the two base pairs in stem-II were disrupted (Fig. 2a). As shown in Fig. 2(b), accumulation of these mutants was approximately 100-fold less than wild-type (wt). At a 10^6-fold dilution, the wt fragment was hardly visible any more (data not shown). Accumulation of M2 gRNA, which was designed to restore the four disrupted base pairs of M1, was also severely compromised. This may be due to the formation of an alternative structure in M2 having altered IL and AL sequences (Fig. 2a). The importance of the loop sequences was assessed by mutants M3, M4 and M7. The gRNA of these three mutants also accumulated up to 100-fold less than wt did. Mutant M5, in which the C : C and C : A mismatches in IL-II were substituted with an A : U and G : C bp, respectively (Fig. 2a), showed a rather mild reduction in gRNA accumulation (Fig. 2b). Similar results have been reported for TYMV, where substituting protonatable C : C and C : A mismatches by Watson–Crick base pairs was tolerated *in vivo*, although spontaneous revertants were found to have partially recovered mismatches after several rounds of infection (Hellendoorn *et al.*, 1997; Bink *et al.*, 2002).

Since mutagenesis has previously been carried out in the corresponding region of negative-strand RNA (Fig. 2c; Lin *et al.*, 2005), it is of interest to address how these substitutions interfered with the secondary structure of our model for positive-strand RNA. We note that, in the region which forms critical structures in both positive- and negative-strand RNA, double mutations that were designed for maintaining structures in one strand may seriously disrupt structures present in the other strand. For instance, the unexpected decrease in the accumulation of our mutant M2 may also be attributed to alterations in the proposed negative-strand hairpins (Lin *et al.*, 2005). Likewise, the surprisingly low replication observed by Lin *et al.* (2005) of the double mutant (BaLSR), which was designed to restore the stem of a hairpin in negative-strand RNA, could be the result of disrupting stem-I and stem-III in positive-strand RNA (Fig. 2a).

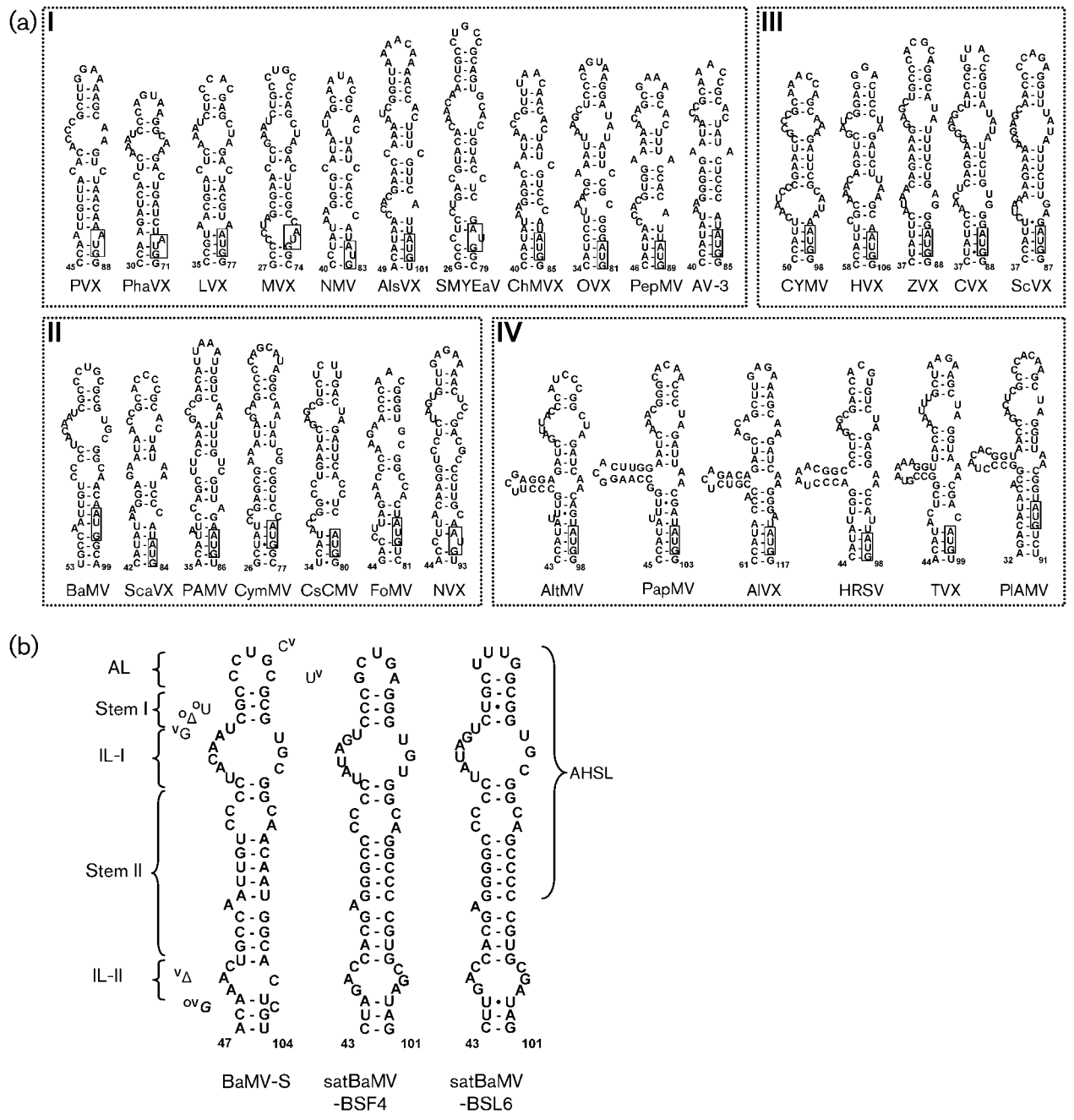

Fig. 3. Homologous structures in the 5′-proximal sequence of potexviruses and BaMV satellites. (a) Putative hairpins around the AUG of ORF1 of potexviruses were predicted by Mfold and grouped into four types (I–IV) as described in the text. Sequences shown are potato virus X (PVX) (NC_011620.1), phaius virus X (PhaVX) (NC_010295.1), lily virus X (LVX) (NC_007192.1), mint virus X (MVX) (NC_006948.1), narcissus mosaic virus (NMV) (NC_001441.1), *Alstroemeria* virus X (AlsVX) (NC_007408.1), strawberry mild yellow edge-associated virus (SMYEaV) (NC_003794.1), *Chenopodium* mosaic virus X (ChMVX) (NC_008251.1), *Opuntia* virus X (OVX) (NC_006060.1), pepino mosaic virus (PepMV) (NC_004067.1), asparagus virus 3 (AV-3) (NC_010416.1), bamboo mosaic virus (BaMV) (AF018156.1), scallion virus X (ScaVX) (NC_003400.1), potato aucuba mosaic virus (PAMV) (NC_003632.1), *Cymbidium* mosaic virus (CymMV) (NC_001812.1), cassava common mosaic virus (CsCMV) (NC_001658.1), foxtail mosaic virus (FoMV) (NC_001483.1), clover yellow mosaic virus (CYMV) (NC_001753.1), *Hosta* virus X (HVX) (NC_011544.1), *Zygocactus* virus X (ZVX) (NC_006059.1), cactus virus X (CVX) (NC_002815.2), *Nerine* virus X (NVX) (NC_007679.1), *Schlumbergera* virus X (ScVX) (NC_011659.1), papaya mosaic virus (PapMV) (NC_001748.1), *Allium* virus X (AlVX) (NC_012211.1), *Hydrangea* ringspot virus (HRSV) (NC_006943.1), tulip virus X (TVX) (NC_004322.1), *Plantago asiatica* mosaic virus (PlAMV) (NC_003849.1) and *Alternanthera* mosaic virus (AltMV) (NC_007731.1). (b) Structural homology between the 5′-proximal sequences of BaMV and satellite RNAs. Sequence variations between BaMV strains S, V and the satRNA-free strain O are indicated. Secondary structures of the apical hairpin stem–loop (AHSL) in the two model satRNAs, BSF4 and BSL6, are shown (adapted from Chen *et al.*, 2007a).

Given the functional importance of this hairpin for BaMV accumulation, homologues in other potexvirus RNAs were investigated. Similar stem–loop structures containing the start codon of ORF1 were predicted by Mfold in the 5′UTR of all potexviruses. These homologues can be clustered into four distinct types according to their structural features (Fig. 3a). Type I is characterized by possession of a single mismatch (C : C, A : A or A : C) in stem-II. The homologue identified in potato virus X (PVX), whose secondary structure is supported by experimental and phylogenetic data (Miller *et al.*, 1998, 1999), is assigned to this type; type II hairpins resemble the secondary structure of BaMV with tandem or triple mismatches in stem-II; type III hairpins consist of an additional IL in stem-II; and type IV is characterized by an additional hairpin in stem-II.

With the exception of PVX and BaMV, there are no experimental data for the hairpins of the other potexviruses. For BaMV, a previous study of the corresponding region focused on *cis*-acting elements in negative-strand RNA (Lin *et al.*, 2005). For PVX, the sequence of AL, IL-I and the C : C mismatch were shown to be critical for gRNA accumulation (Miller *et al.*, 1998, 1999), although a C : A mismatch was temporarily functional (Miller *et al.*, 1999). The C : C mismatch has also been implicated in coat protein binding (Kwon *et al.*, 2005) and cell-to-cell movement (Lough *et al.*, 2006). In the 5′UTR of another group of plant viruses, e.g. TYMV, *cis*-acting elements that consist of the consecutive C : C and C : A mismatches were found upstream or overlapping with the first AUG (Hellendoorn *et al.*, 1997). These mismatches have been shown to be important for encapsidation and it has been suggested that they are protonated at a pH of 5.0 (Bink *et al.*, 2002). Thus, the C : C and C : A mismatches in the BaMV 5′ element may also be protonatable under acidic conditions and be involved in encapsidation.

A unique feature of BaMV among the potexviruses is its possession of satRNAs (Lin & Hsu, 1994). There is no sequence homology between the various satRNAs and BaMV except for the presence of an A-rich leader sequence at the 5′ end in both BaMV and satBaMV RNAs. However, the structural homology in the 5′ end is striking (Fig. 3b). Secondary structures of two major types of satRNAs (BSF4 and BSL6) have been determined previously (Annamalai *et al.*, 2003; Chen *et al.*, 2007a). Stem-II is composed of 11 bp in both sat- and helper RNAs, and includes the two conserved C : C and C : A mismatches and the A-bulge at identical positions in this stem.

There are some differences between the three hairpins, particularly in AL and IL-I (Fig. 3b), which may be related to the attenuating effect of satBaMV-BSL6 on BaMV accumulation (Annamalai *et al.*, 2003, Chen *et al.*, 2007a). The BSL6-like satRNA which contains the UUUG sequence in AL was reported to downregulate BaMV replication, while the BSF4-like satRNA which has the GCUGA sequence in AL did not significantly interfere with the replication of helper BaMV (Annamalai *et al.*, 2003). Furthermore, it was recently shown that changing the UGC sequence in satBaMV-BSL6 IL-I to UGU completely abolishes the satRNA-mediated downregulation of helper BaMV gRNA (Chen *et al.*, 2007a). On the other hand, satBaMV-BSF4 was shown to downregulate the replication of helper BaMV when its UGU sequence in IL-I was changed to UGC (Chen *et al.*, 2007a). These results indicated that the BSL6-like IL-I, with the UGC sequence, dominates satRNA-mediated attenuation. Interestingly, BaMV has the BSL6-like UGC loop (Fig. 3b). It is tempting to speculate that competition for a common factor, host and/or viral, that recognizes the internal loop, lies at the basis of this attenuation.

Several BaMV strains, including BaMV-S, BaMV-O, BaMV-L and BaMV40A, have been isolated or generated in the past and used in studies of BaMV biology and satBaMV-mediated regulation (Chang *et al.*, 1997; Hsu *et al.*, 1998; Chen *et al.*, 2005). We note that none of these strain-specific variations is in conflict with the formation of stem-II in positive-strand RNA (Fig. 3a), while some disrupt a previously proposed structure in negative-strand RNA (Lin *et al.*, 2005). Strain-specific variations in BaMV may be responsible for differences in gRNA accumulation, symptom induction and satRNA-mediated interaction, as shown previously (Hsu *et al.*, 1998; Yeh *et al.*, 1999). For instance, satBaMV-BSF4 has been shown to promote formation of local lesions on *Chenopodium quinoa* leaves when co-infected with BaMV-L, a sat-free BaMV derived from BaMV-V which is naturally associated with satRNAs (Lin *et al.*, 1994; Hsu *et al.*, 1998). However, such an effect was not observed in leaves co-infected with BaMV-S, which is the strain derived from BaMV-O that is not associated with satRNAs, according to the literature (Chang *et al.*, 1997; Hsu *et al.*, 1998). Although co-infection of satBaMV-BSL6 reduces lesion formation and gRNA accumulation in both BaMV-S- and BaMV-L-infected leaves (Hsu *et al.*, 1998), it would be interesting to explore the natural helper BaMV of satRNA-BSL6 in the field. This may clarify whether the homology in the 5′ hairpin plays any role in the interaction between satRNA and BaMV.

We conclude that the unique conservations and variations of the 5′ structure between satBaMV and BaMV that we have shown in this study may provide novel insights into helper–satellite interactions in BaMV and other viruses (Simon *et al.*, 2004).

Acknowledgements

We acknowledge Oumou Maiga and Elodie Tenconi for their initial contributions, and N. S. Lin for the gift of plasmid pBaMV. This research was supported by a VIDI grant from the Netherlands Organization for Scientific Research (NWO) to R. C. L. O.

References

Annamalai, P., Hsu, Y. H., Liu, Y. P., Tsai, C. H. & Lin, N. S. (2003). Structural and mutational analyses of *cis*-acting sequences in the

5′-untranslated region of satellite RNA of bamboo mosaic potexvirus. *Virology* **311**, 229–239.

Bink, H. H. J., Hellendoorn, K., van der Meulen, J. & Pleij, C. W. A. (2002). Protonation of non-Watson–Crick base pairs and encapsidation of turnip yellow mosaic virus RNA. *Proc Natl Acad Sci U S A* **99**, 13465–13470.

Chang, B. Y., Lin, N. S., Liou, D. Y., Chen, J. P., Liou, G. G. & Hsu, Y. H. (1997). Subcellular localization of the 28 kDa protein of the triple-gene-block of bamboo mosaic potexvirus. *J Gen Virol* **78**, 1175–1179.

Chen, I. H., Chou, W. J., Lee, P. Y., Hsu, Y. H. & Tsai, C. H. (2005). The AAUAAA motif of bamboo mosaic virus RNA is involved in minus-strand RNA synthesis and plus-strand RNA polyadenylation. *J Virol* **79**, 14555–14561.

Chen, H. C., Hsu, Y. H. & Lin, N. S. (2007a). Downregulation of *Bamboo mosaic virus* replication requires the 5′ apical hairpin stem loop structure and sequence of satellite RNA. *Virology* **365**, 271–284.

Chen, S. C., van den Born, E., van den Worm, S. H., Pleij, C. W. A., Snijder, E. J. & Olsthoorn, R. C. L. (2007b). New structure model for the packaging signal in the genome of group IIa coronaviruses. *J Virol* **81**, 6771–6774.

Cheng, C. P. & Tsai, C. H. (1999). Structural and functional analysis of the 3′ untranslated region of bamboo mosaic potexvirus genomic RNA. *J Mol Biol* **288**, 555–565.

Cheng, J. H., Peng, C. W., Hsu, Y. H. & Tsai, C. H. (2002). The synthesis of minus-strand RNA of bamboo mosaic potexvirus initiates from multiple sites within the poly(A) tail. *J Virol* **76**, 6114–6120.

Hellendoorn, K., Verlaan, P. W. & Pleij, C. W. A. (1997). A functional role for the conserved protonatable hairpins in the 5′ untranslated region of turnip yellow mosaic virus RNA. *J Virol* **71**, 8774–8779.

Hsu, Y. H., Lee, Y. S., Liu, J. S. & Lin, N. S. (1998). Differential interactions of bamboo mosaic potexvirus satellite RNAs, helper virus, and host plants. *Mol Plant Microbe Interact* **11**, 1207–1213.

Huang, C. Y., Huang, Y. L., Meng, M., Hsu, Y. H. & Tsai, C. H. (2001). Sequences at the 3′ untranslated region of bamboo mosaic potexvirus RNA interact with the viral RNA-dependent RNA polymerase. *J Virol* **75**, 2818–2824.

Kwon, S. J., Park, M. R., Kim, K. W., Plante, C. A., Hemenway, C. L. & Kim, K. H. (2005). *cis*-Acting sequences required for coat protein binding and *in vitro* assembly of *Potato virus X*. *Virology* **334**, 83–97.

Lin, N. S. & Hsu, Y. H. (1994). A satellite RNA associated with bamboo mosaic potexvirus. *Virology* **202**, 707–714.

Lin, N. S., Lin, B. Y., Lo, N. W., Hu, C. C., Chow, T. Y. & Hsu, Y. H. (1994). Nucleotide sequence of the genomic RNA of bamboo mosaic potexvirus. *J Gen Virol* **75**, 2513–2518.

Lin, M. K., Chang, B. Y., Liao, J. T., Lin, N. S. & Hsu, Y. H. (2004). Arg-16 and Arg-21 in the N-terminal region of the triple-gene-block protein 1 of *Bamboo mosaic virus* are essential for virus movement. *J Gen Virol* **85**, 251–259.

Lin, J. W., Chiu, H. N., Chen, I. H., Chen, T. C., Hsu, Y. H. & Tsai, C. H. (2005). Structural and functional analysis of the *cis*-acting elements required for plus-strand RNA synthesis of *Bamboo mosaic virus*. *J Virol* **79**, 9046–9053.

Lough, T. J., Lee, R. H., Emerson, S. J., Forster, R. L. & Lucas, W. J. (2006). Functional analysis of the 5′ untranslated region of potexvirus RNA reveals a role in viral replication and cell-to-cell movement. *Virology* **351**, 455–465.

Lowman, H. B. & Draper, D. E. (1986). On the recognition of helical RNA by cobra venom V1 nuclease. *J Biol Chem* **261**, 5396–5403.

Miller, E. D., Plante, C. A., Kim, K. H., Brown, J. W. & Hemenway, C. (1998). Stem-loop structure in the 5′ region of potato virus X genome required for plus-strand RNA accumulation. *J Mol Biol* **284**, 591–608.

Miller, E. D., Kim, K. H. & Hemenway, C. (1999). Restoration of a stem-loop structure required for potato virus X RNA accumulation indicates selection for a mismatch and a GNRA tetraloop. *Virology* **260**, 342–353.

Simon, A. E., Roossinck, M. J. & Havelda, Z. (2004). Plant virus satellite and defective interfering RNAs: new paradigms for a new century. *Annu Rev Phytopathol* **42**, 415–437.

Tsai, C. H., Cheng, C. P., Peng, C. W., Lin, B. Y., Lin, N. S. & Hsu, Y. H. (1999). Sufficient length of a poly(A) tail for the formation of a potential pseudoknot is required for efficient replication of bamboo mosaic potexvirus RNA. *J Virol* **73**, 2703–2709.

Yeh, T. Y., Lin, B. Y., Chang, Y. C., Hsu, Y. H. & Lin, N. S. (1999). A defective RNA associated with bamboo mosaic virus and the possible common mechanisms for RNA recombination in potexviruses. *Virus Genes* **18**, 121–128.

Zuker, M. (2003). Mfold web server for nucleic acid folding and hybridization prediction. *Nucleic Acids Res* **31**, 3406–3415.